AIE in the Halogenated Anils and their Utilization as Fluorescent Probes for Explosive Nitro-aromatics

Aadil A. Ahangar, Ishtiyaq Ahmad and Aijaz A. Dar,*

Department of Chemistry, Inorganic Section, University of Kashmir, Hazratbal, Srinagar-190006, India.

Electronic Supporting Information

Figure ESI-1: TGA /DTA curve of molecular solid **1.**
Figure ESI-2: TGA/DTA curve of molecular solid **2.**
Figure ESI-3: TGA /DTA curve of molecular solid **3.**
Figure ESI-4: FT-IR Spectrum of **1**.
Figure ESI-5: FT-IR Spectrum of **2**.
Figure ESI-6: FT-IR Spectrum of **3**.
Figure ESI-7: Molecular structure depicting slipped π-stacking interaction in 1.
Figure ESI-8: Molecular structure depicting centrosymmetric π-stacking overlap in **2**.
Figure ESI-9: Molecular structure represents formation of 2D-sheets via π-stacking overlap in **3**.
Figure ESI-10: d_{norm} surface of molecular solid 1.
Figure ESI-11: d_{norm} surface of molecular solid 2.
Figure ESI-12: d_{norm} surface of molecular solid 3.
Figure ESI-13: Curvedness surface of molecular solid **1.**
Figure ESI-14: Curvedness surface of molecular solid **2.**
Figure ESI-15: Curvedness surface of molecular solid **3.**
Figure ESI-16: Shape-index surface of molecular solid **1.**
Figure ESI-17: Shape-index surface of molecular solid **2.**
Figure ESI-18: Shape-index surface of molecular solid **3.**
Table 1: Quantification of σ-hole formation in the molecular solids **1-3.**
Figure ESI-19: Individual fingerprint plot of molecular solid **1.**
Figure ESI-20: Individual fingerprint plot of molecular solid **2.**
Figure ESI-21: Individual fingerprint plot of molecular solid **3.**
Figure ESI-22: Framework analysis of molecular solid **1**.
Figure ESI-23: Framework analysis of molecular solid **2.**
Figure ESI-24: Framework analysis of molecular solid **3.**
Figure ESI-25: Absorption spectrum of molecular solid **1.**
Figure ESI-26: Absorption spectrum of molecular solid **2.**
Figure ESI-27: Absorption spectrum of molecular solid **3.**
Figure ESI-28: Tauc-plot of molecular solid **1-3.**
Figure ESI-29: Emission spectra depicting AIE behaviour of **2.**
Figure ESI-30: Emission spectra depicting AIE behaviour of **3.**
Figure ESI-31: Histogram depicting AIE behaviour of **2.**
Figure ESI-32: Histogram depicting AIE behaviour of **3.**
Figure ESI-33: DLS plot validating AIE behaviour of **2.**
Figure ESI-34: DLS plot validating AIE behaviour of **3.**
Figure ESI-35: Emission plot validating quenching behaviour of picric acid by AIE system **2.**
Figure ESI-36: Emission plot validating quenching behaviour of picric acid by AIE system **3.**
Figure ESI-37: Emission plot validating quenching behaviour of O-Nitrobenzaldehyde by AIE system **2.**
Figure ESI-38: Emission plot validating quenching behaviour of p-Nitrobenzaldehyde by AIE system **2.**
Figure ESI-39: Emission plot validating quenching behaviour of 2,4-dinitrobenzaldehyde by AIE system **2.**

Table ESI-2: The binding constant, stern-Volmer constant, and limit of detection values of AIE system -2nd(in presence of various interfering agents) titrated against P.A are shown below.

Figure ESI-40: PL-spectra showing P.A. sensing by AIEgen **2** polluted with detergent solution and histogram showing comperative peak intensity values at different concentrations of P.A.

Figure ESI-41: PL-spectra showing P.A. sensing by AIEgen **2** polluted with commercial perfume and histogram showing comperative peak intensity values at different concentrations of P.A.

Figure ESI-42: PL-spectra showing P.A. sensing by AIEgen **2** polluted with alchol and histogram showing comperative peak intensity values at different concentrations of P.A.

Figure ESI-43: PL-spectra showing P.A. sensing by AIEgen **2** polluted with lake water solution and histogram showing comperative peak intensity values at different concentrations of P.A.

TGA/DTA PLOTS OF 1-3

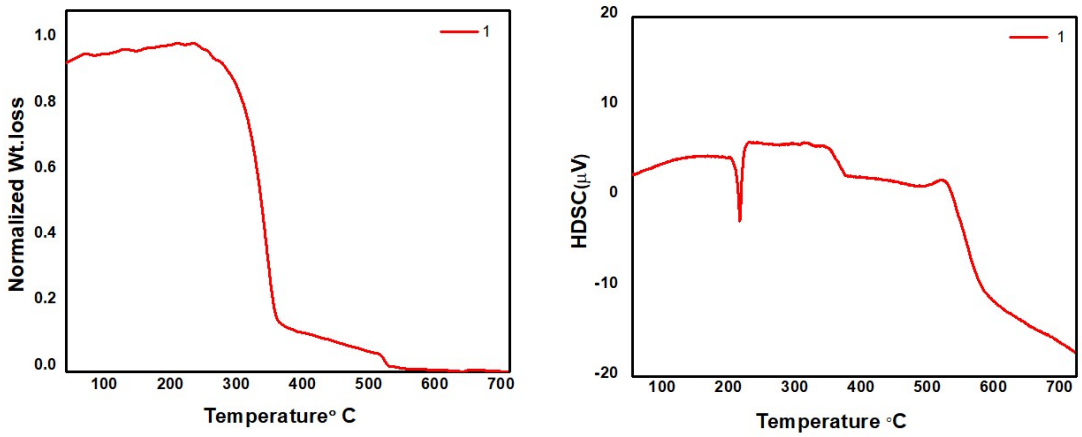

Figure ESI-1: TGA/DTA curve of molecular solid **1.**

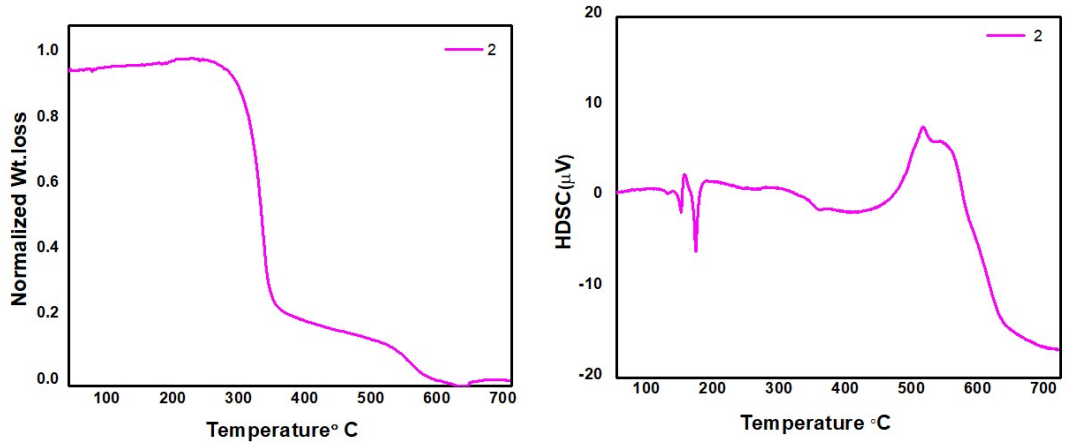

Figure ESI-2: TGA/DTA curve of molecular solid **2.**

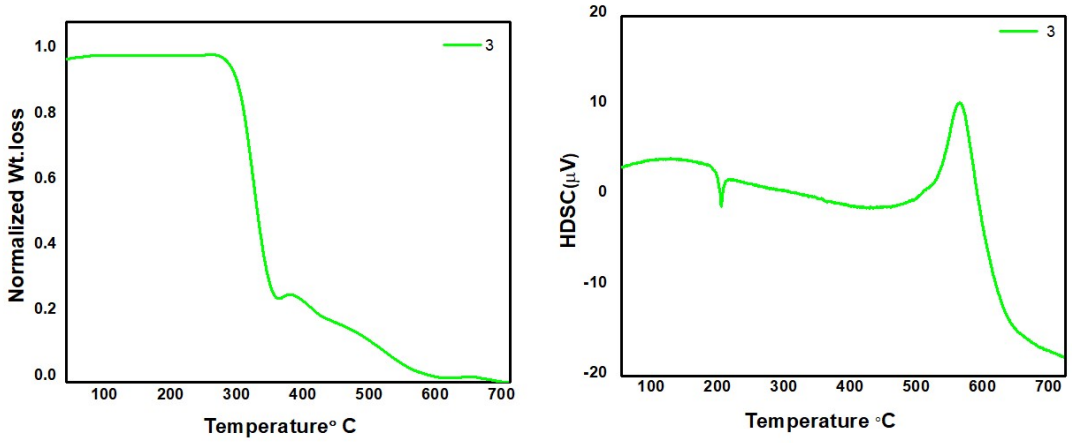

Figure ESI-3: TGA /DTA curve of molecular solid **3.**

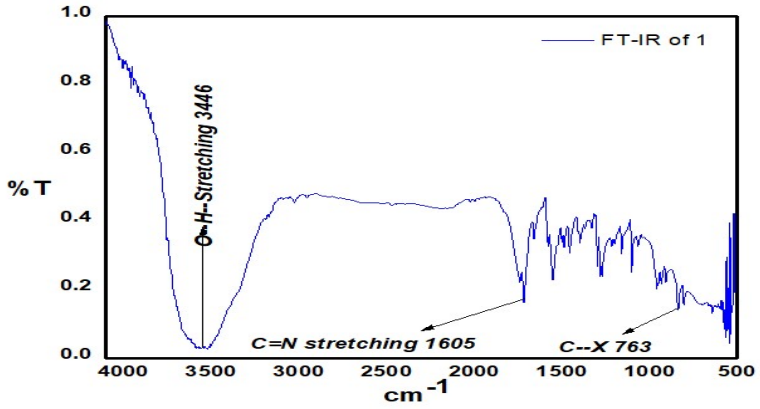

Figure ESI-4:FT-IR Spectrum of **1.**

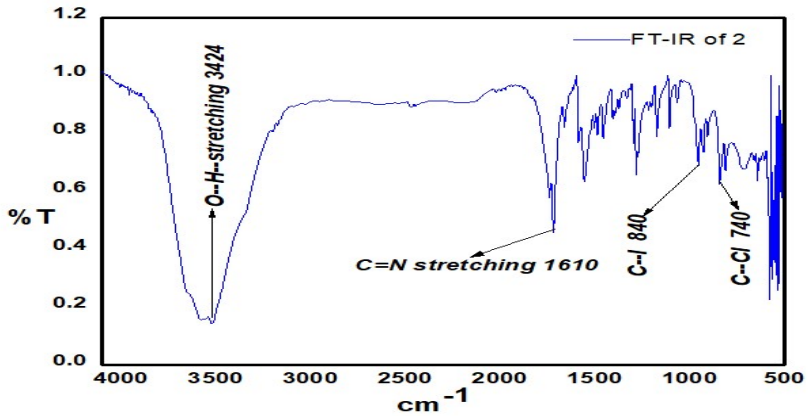

Figure ESI-5:FT-IR Spectrum of **2.**

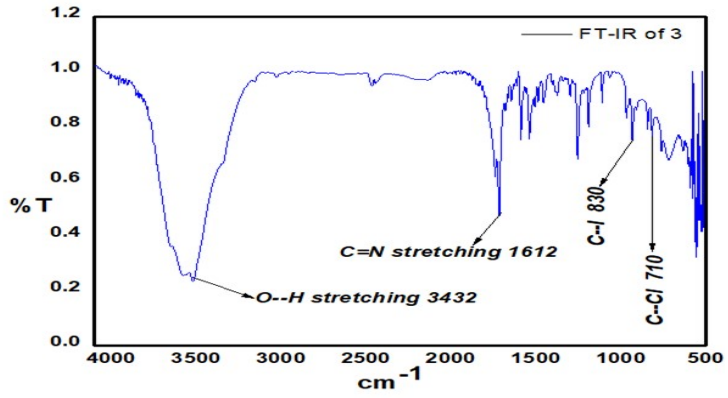

Figure ESI-6:FT-IR Spectrum of **3**.

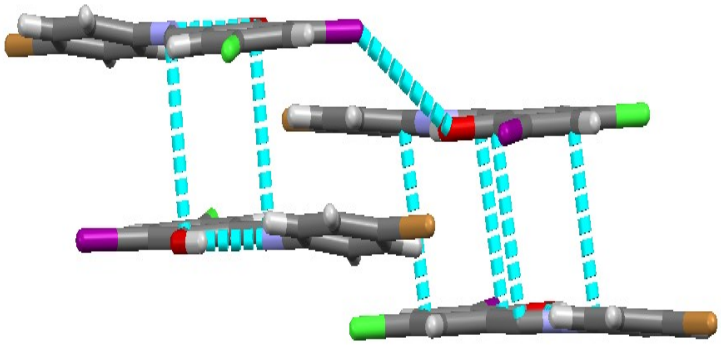

Figure ESI-7: Molecular structure depicting slipped π-stacking interaction in 1.

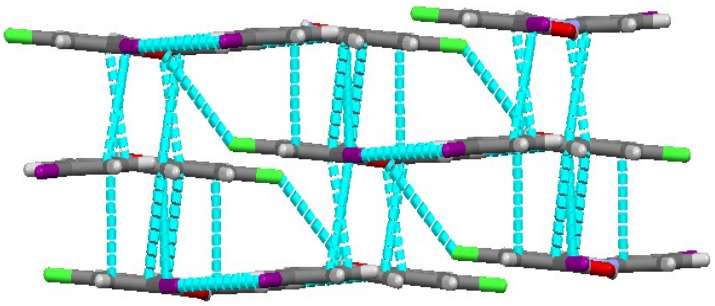

Figure ESI-8: Molecular structure depicting centro-symmetric π-stacking overlap in **2**.

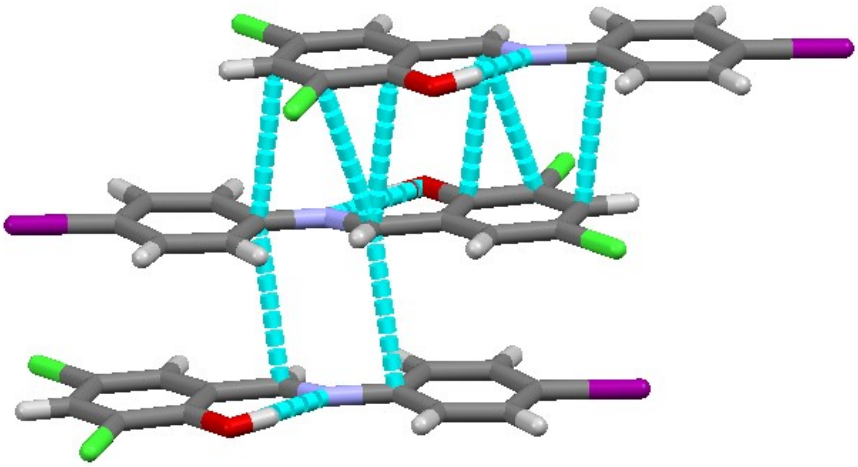

Figure ESI-9: Molecular structure represents formation of 2D-sheets via π-stacking overlap in **3**.

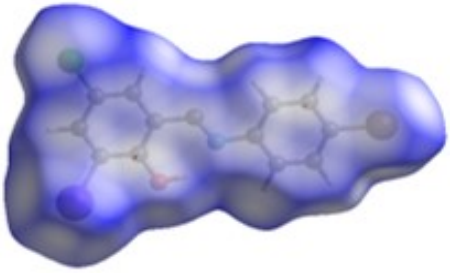

Figure ESI-10: d_{norm} surface of molecular solid **1**.

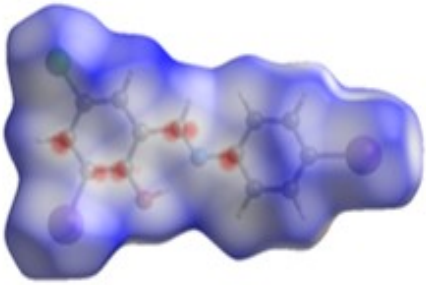

Figure ESI-11: d_{norm} surface of molecular solid **2**.

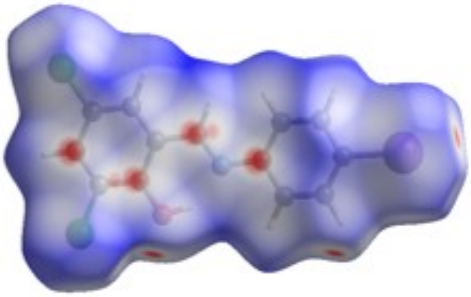

Figure ESI-12: d_{norm} surface of molecular solid **3.**

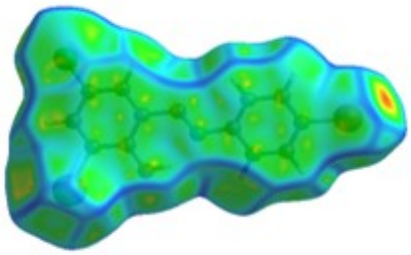

Figure ESI-13: Curvedness surface of molecular solid **1.**

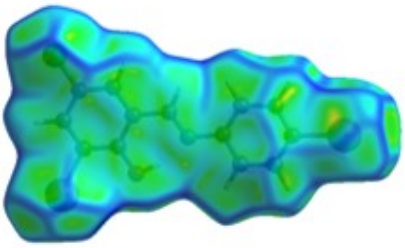

Figure ESI-14: Curvedness surface of molecular solid **2.**

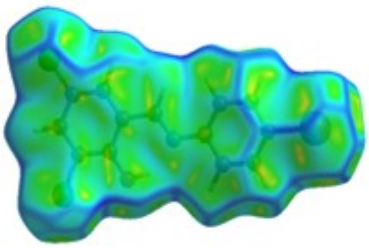

Figure ESI-15: Curvedness surface of molecular solid **3.**

The d_{norm} surface gives insight about the nature of supramolecular interactions exhibited by molecular solids differentiated by three different colours such as red, blue and white .The red spots indicate those intermolecular interactions which are short, strong and are usually shown by electronegative atoms, while colour represent moderate intermolecular interaction which are usually shown by the middle portion of dnorm surface involved in π-π interactions, while the very weak contacts are shown by blue coded colour and are mostly dominated around the periphery portion of dnorm surface where the presence of halogen atoms is dominated. Further insights about the strong π-π interactions is provided by Curvedness , the almost flat surface of these molecular solids represents the extensive π-π interactions in them.

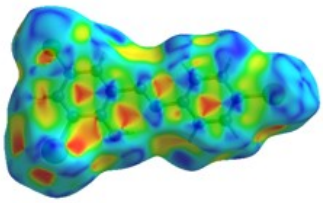

Figure ESI-16: Shape-index surface of molecular solid **1.**

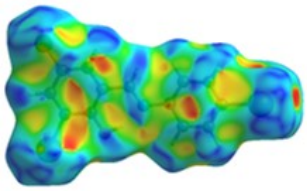

Figure ESI-17: Shape-index surface of molecular solid **2.**

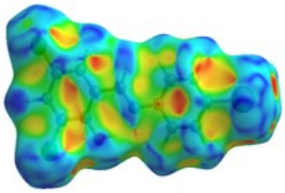

Figure ESI-18: Shape-index surface of molecular solid **3.**

Table ESI-1: Quantification of σ-hole formation in the molecular solids **1-3.**

Halogen atom	Electrostatic Potential value (a.u.)	Sigma hole formation.
Molecular solid 1		
Br1	**0.0020**	**Yes**
I2	**0.0006**	**Yes**
Cl3	**-0.0177**	**No**
Molecular solid 2		
I1	**0.0107**	**Yes**
I2	**0.0056**	**Yes**
Cl3	**-0.0192**	**No**
Molecular solid 3		
I1	**0.0154**	**Yes**
Cl2	**-0.0221**	**No**
Cl3	**-0.0161**	**No**

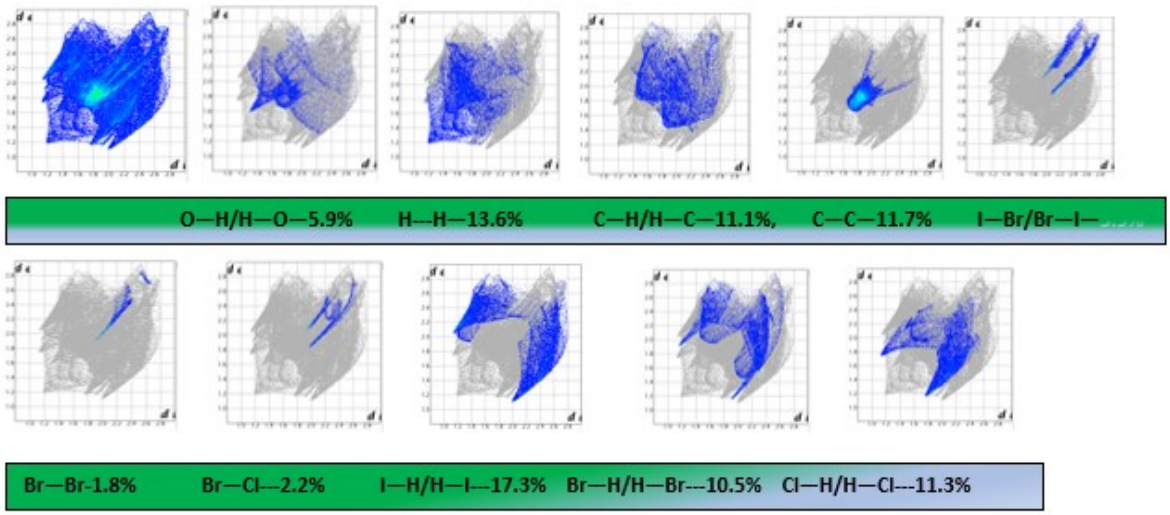

Figure ESI-19: Fingerprint plots representing quantification of intermolecular interactions in **1.**

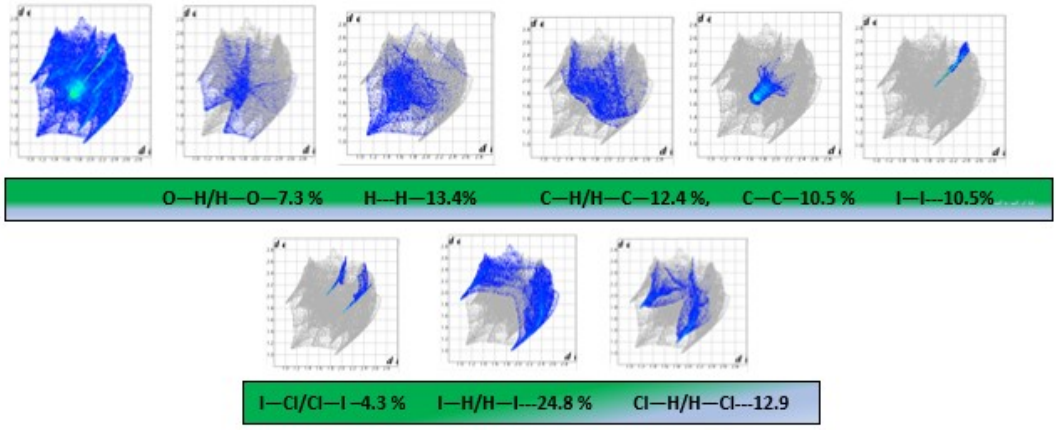

Figure ESI-20: Fingerprint plots representing quantification of intermolecular interactions in **2.**

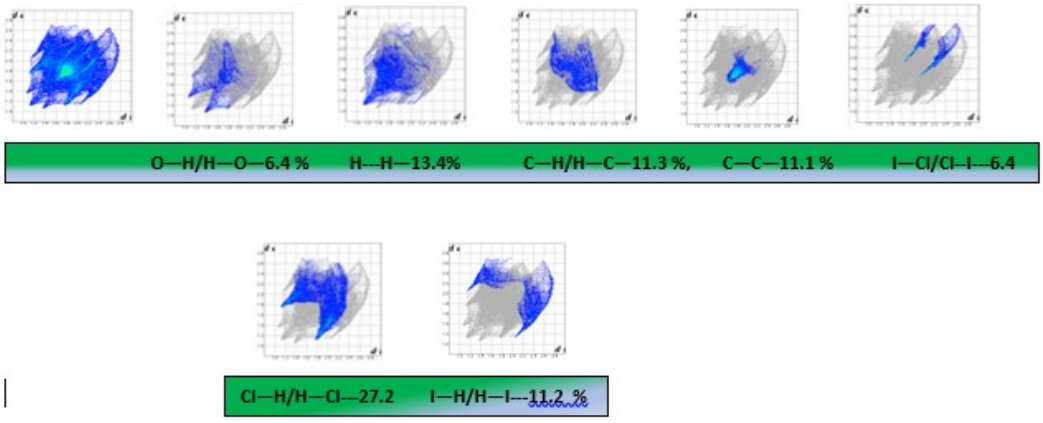

Figure ESI-21: Fingerprint plots representing quantification of intermolecular interactions in **3.**

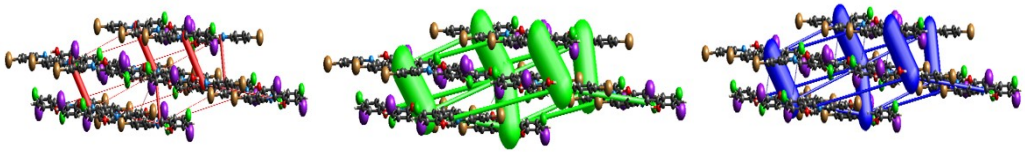

Figure ESI-22: Framework analysis of molecular solid 1.

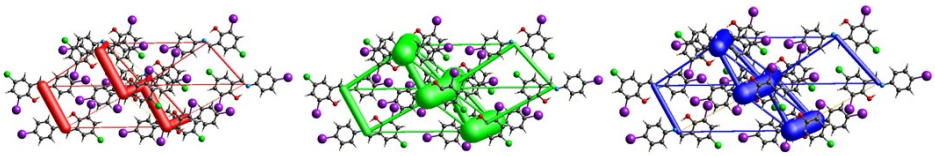

Figure ESI-23: Framework analysis of molecular solid 2.

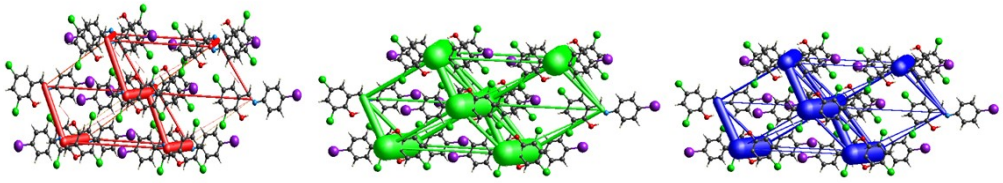

Figure ESI-24: Framework analysis of molecular solid 3.

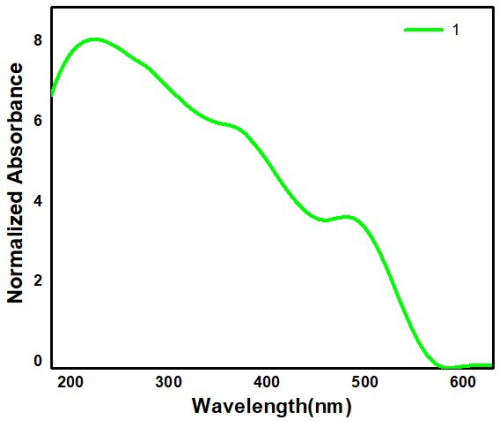

Figure ESI-25: Absorption spectrum of molecular solid **1.**

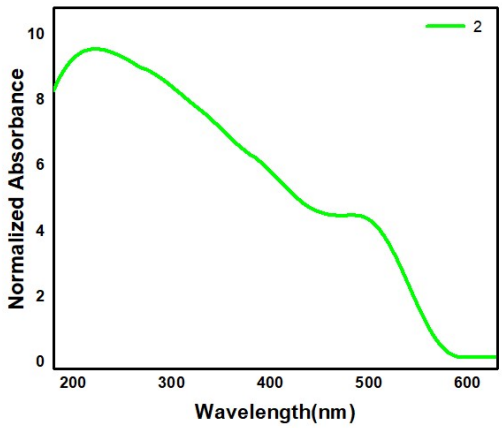

Figure ESI-26: Absorption spectrum of molecular solid **2.**

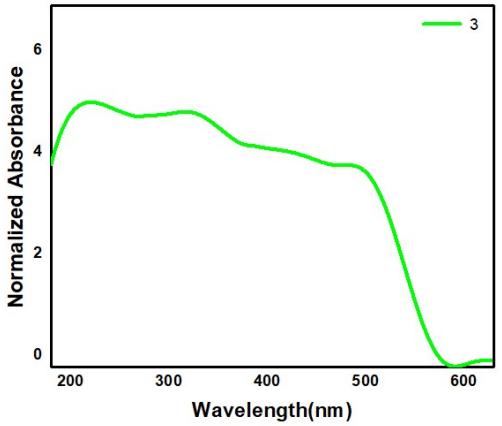

Figure ESI-27: Absorption spectrum of molecular solid **3.**

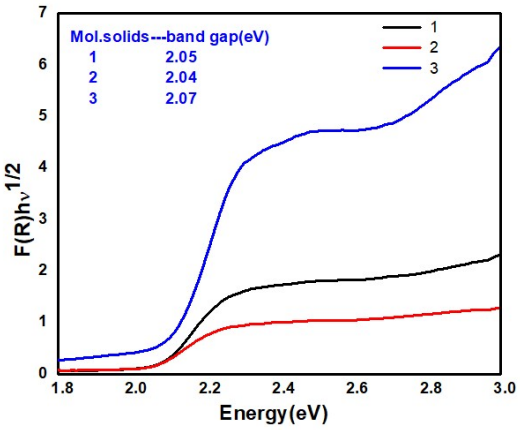

Figure ESI-28: Tauc-plot of molecular solid **1-3.**

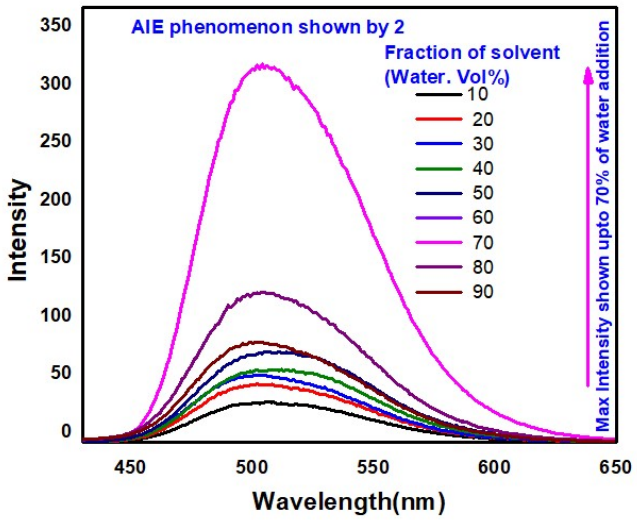

Figure ESI-29: Emission spectra depicting AIE behaviour of **2.**

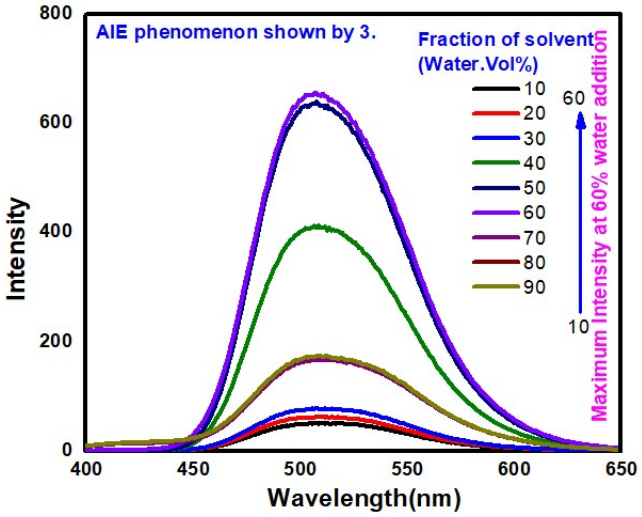

Figure ESI-30: Emission spectra depicting AIE behaviour of **3.**

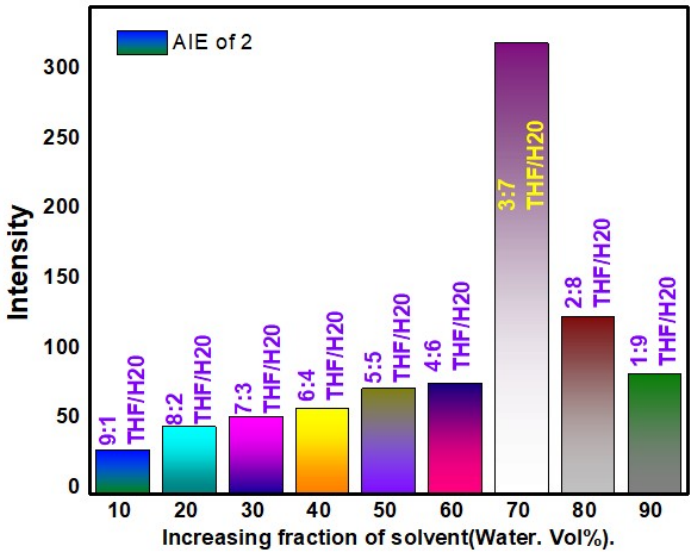

Figure ESI-31: Histogram depicting AIE behaviour of **2.**

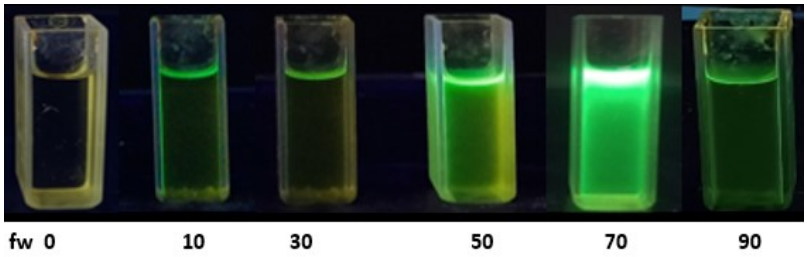

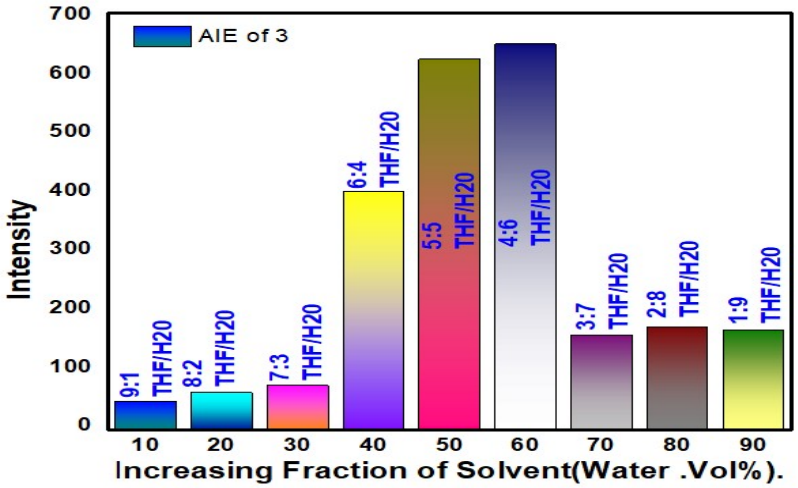

Figure ESI-32: Optical images and DLS histogram depicting AIE behaviour of **3.**

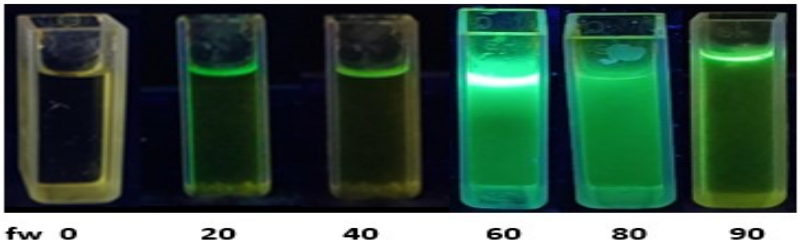

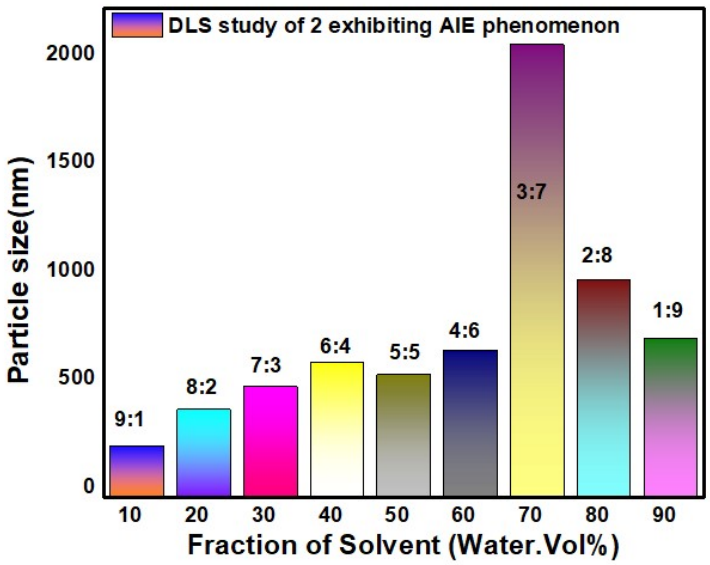

Figure ESI-33: Optical images and DLS histogram validating AIE behaviour of **2.**

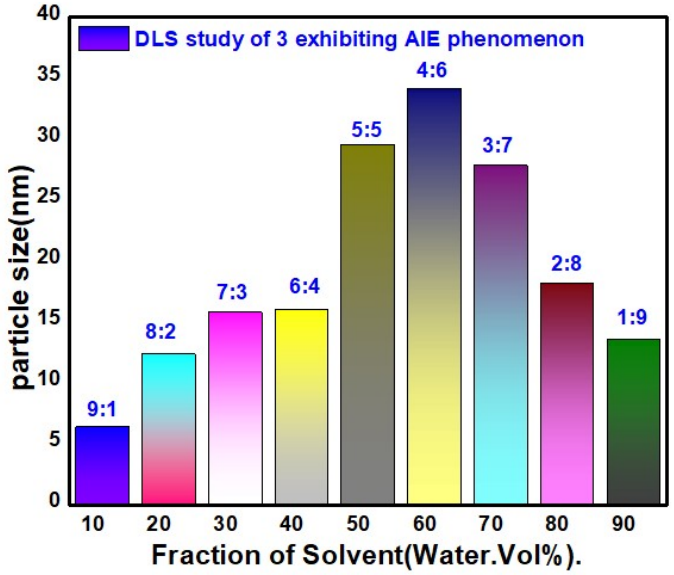

Figure ESI-34: DLS plot validating AIE behaviour of **3.**

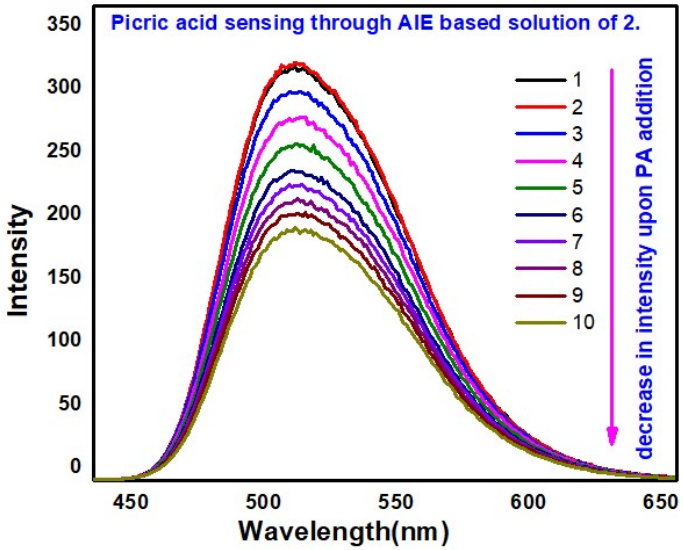

Figure ESI-35: Emission plot validating quenching behaviour of picric acid by AIE system **2.**

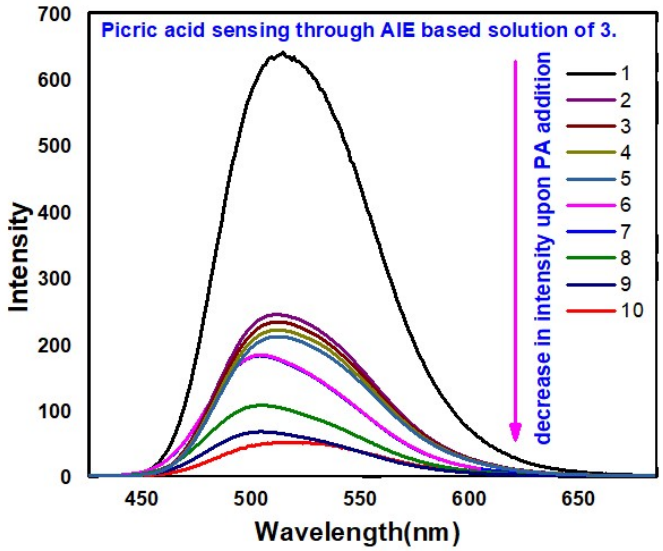

Figure ESI-36: Emission plot validating quenching behaviour of picric acid by AIE system **3.**

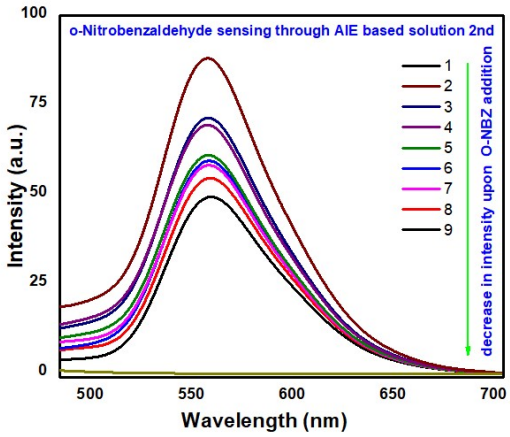

Figure ESI-37: Emission plot validating quenching behaviour of O-Nitrobenzaldehyde by AIE system **2.**

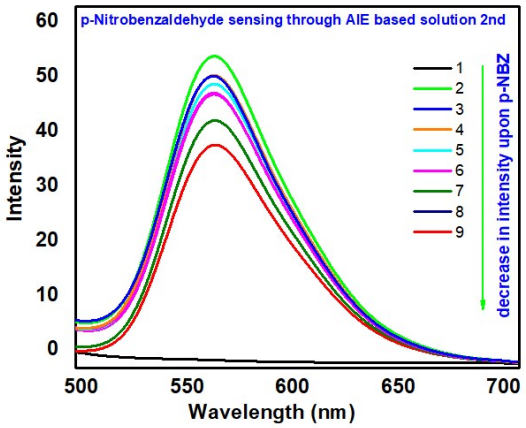

Figure ESI-38: Emission plot validating quenching behaviour of p-Nitrobenzaldehyde by AIE system **2.**

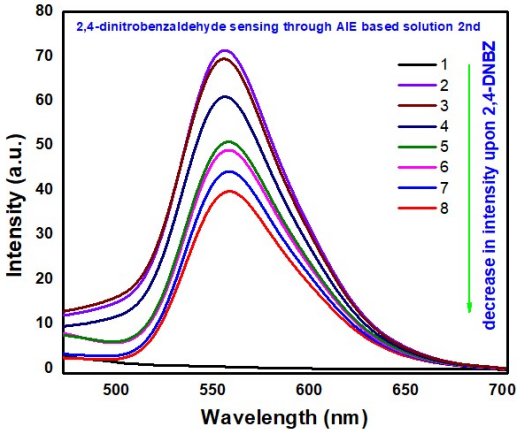

Figure ESI-39: Emission plot validating quenching behaviour of 2,4-dinitrobenzaldehyde by AIE system **2.**

Interference study

Interference study

The interference study was carried out on a spectrofluorimeter to check the selectivity of Nitro-aromatics (P.A.) utilizing the AIEgen in the presence of interfering agents. Various interfering agents of daily use such as detergent, perfume, alcohol and polluted water were selected to study their influence on the sensing behavior of nitro-compound through AIE-system. The AIEgen **2** was selected for performing the interfering study as the system yielded a better binding constant and lower L.O.D. value. During the studies, the titration of picric acid has been carried out in presence of different interfering agents separately. Initially, the PL spectra was recorded for AIEgen **2**, and then 500 µL of interfering agents were added and PL spectra were recorded again. The titration of the resultant polluted solutions of AIEgen 2, was carried with P.A. on similar lines as done for quenching studies with the pure form of AIEgen **2**. 100 µL of $1x10^{-3}$ solution of P.A. was added at each titration step and the titration was followed spectroscopically, until a saturation quenching point was attained.
The interference estudies indicate that the sensing of P.A. by AIEgen **2** is not affected by the presence of pollutants and the binding constant, Ksv constants and L.O.D values are comparable, Table ESI-2, and Figure ESI-40-43, below:

Table ESI-2: The binding constant, Stern-Volmer constant, and limit of detection values of AIEgen-**2** (in presence of various interfering agents) titrated against P.A.

System	P.A. Conc.	Interfering Agents	Binding Constant (K)	Equivalents of P.A titrated.	K_{sv}	L.O.D Value
AIEgen -2	1 x 10^{-3} M	None	5.7x10^{3} M^{-1}	33.8	5.3 x 10^{3}	34 µM
AIEgen -2	1 x 10^{-3} M	Detergent	3.9x 10^{3} M^{-1}	59.8	4.1 x 10^{3} M^{-1}	31 µM
AIEgen -2	1 x 10^{-3} M	Perfume	4.2x 10^{3} M^{-1}	54.94	4.4 x 10^{3} M^{-1}	33 µM
AIEgen -2	1 x 10^{-3} M	Alcohol	3.6x $10^{3}$$M^{-1}$	55.55	3.7x 10^{3} M^{-1}	28.5 µM
AIEgen -2	1 x 10^{-3} M	Lake water	3.8x 10^{3} M^{-1}	57.22	3.6x 10^{3} M^{-1}	29 µM

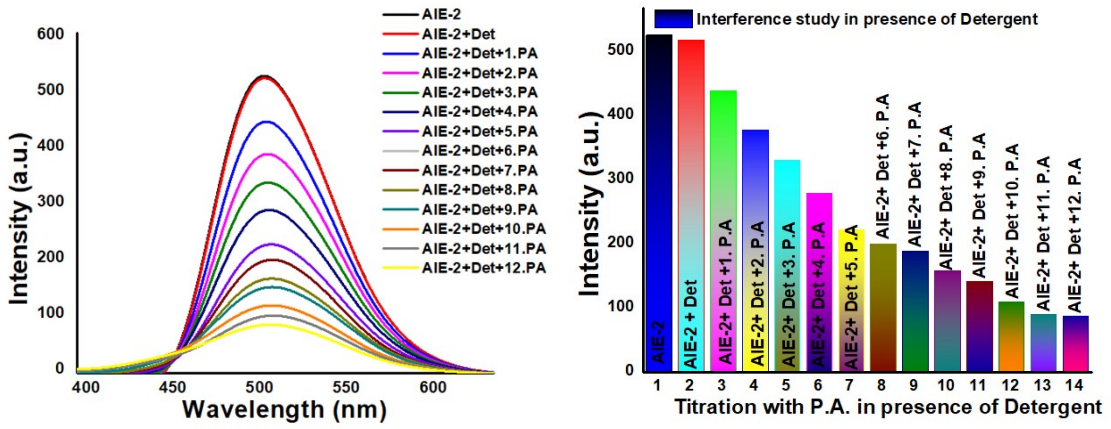

Figure ESI-40: PL-spectra showing P.A. sensing by AIEgen **2** polluted with detergent solution and histogram showing comperative peak intensity values at different concentrations of P.A.

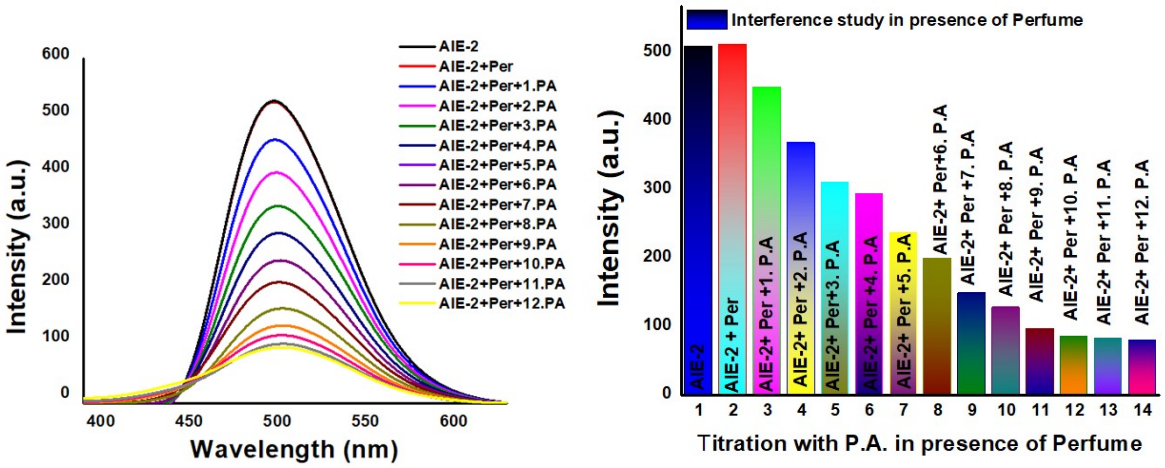

Figure ESI 41: PL-spectra showing P.A. sensing by AIEgen **2** polluted with commercial perfume and histogram showing comperative peak intensity values at different concentrations of P.A.

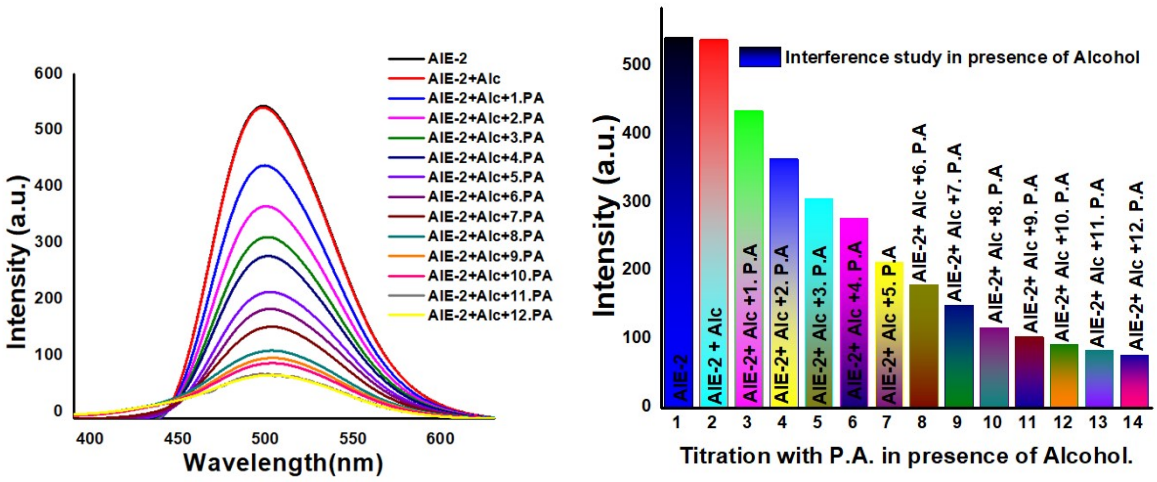

Figure ESI-42: PL-spectra showing P.A. sensing by AIEgen **2** polluted with alchol and histogram showing comperative peak intensity values at different concentrations of P.A.

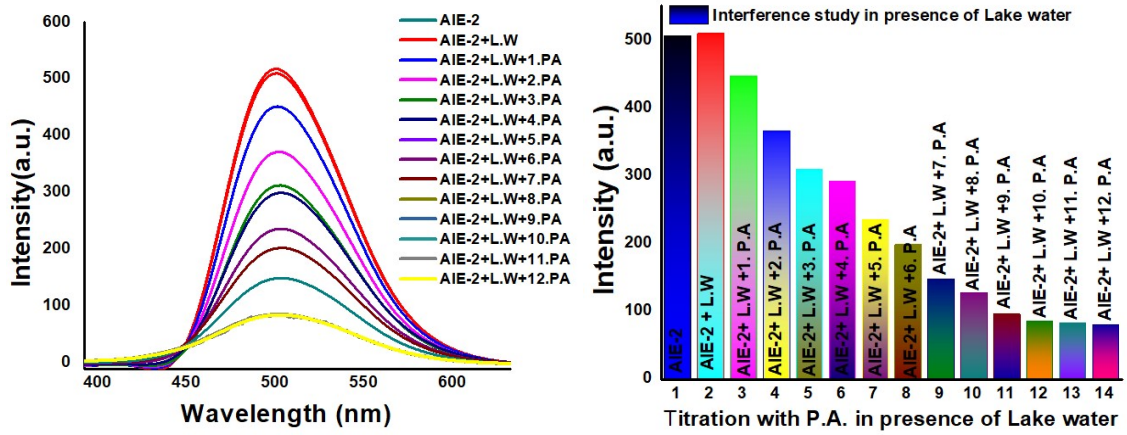

Figure ESI-43: PL-spectra showing P.A. sensing by AIEgen **2** polluted with lake water solution and histogram showing comperative peak intensity values at different concentrations of P.A.

Methodology:

The AIEgen 2 (THF/H20 Solvent system; fw 90) having a concentration of 1x10-3 M was selected for the interference study. The PL spectra of AIEgen 2 were recorded at the excitation wavelength of 365 nm. Initially the 2 mL of the AIEgen 2 was taken in a cuvette for which PL-spectra was recorded. To this solution, 500 μL of a solution of ist interfering agents (i-iv (details given below)) were added and the spectra were recorded again. Then, to the resultant solution aromatic nitro-compound (P.A) of concentration of 1x10-3 M was titrated upon incremental addition of 100 μL, till a saturation limit was attained.

Source and composition of interfering agents used:

Detergent: Detergent with the brand name Alconox, consisting of a homogeneous blend of sodium linear alkyl-aryl-sulfonates, alcoholic sulfate, phosphate and carbonates was used after the prepration of its 1 x10-3 solutions.

Perfume: The brand name of the perfume used for the experiment is DENVER, and it is composed of Ethyl alcohol denatured, propylene Glycol, aqua, Diethyl Phthalate, and B.H.T. The perfume was used at the commercially available concentration.

Alcohol: Absolute alcohol (Ethanol, S.D. Fine) was used in the commercially available concentration.

Polluted water: The water samples were collected from the Dal-lake, located in heart of Srinagar, Jammu and Kashmir, India. The status of the lake is highly polluted and its water is not fit for drinking.

Abbreviations: Det for Detergent, Per for Perfume, Alc for Alcohol (Ethyl-Alcohol), L.W for lake water, and PL- Photoluminescence